Carbon Nanorings

DOI: 10.1002/anie.201406836

Intercrossed Carbon Nanorings with Pure Surface States as Low-Cost and Environment-Friendly Phosphors for White-Light-Emitting Diodes**

*Xiaoming Li, Yanli Liu, Xiufeng Song, Hao Wang, Haoshuang Gu, and Haibo Zeng**

Abstract: *As an important energy-saving technique, white-light-emitting diodes (W-LEDs) have been seeking for low-cost and environment-friendly substitutes for rare-earth-based expensive phosphors or Pd^{2+}/Cd^{2+}-based toxic quantum dots (QDs). In this work, precursors and chemical processes were elaborately designed to synthesize intercrossed carbon nanorings (IC-CNRs) with relatively pure hydroxy surface states for the first time, which enable them to overcome the aggregation-induced quenching (AIQ) effect, and to emit stable yellow-orange luminescence in both colloidal and solid states. As a direct benefit of such scarce solid luminescence from carbon nanomaterials, W-LEDs with color coordinate at (0.28, 0.27), which is close to pure white light (0.33, 0.33), were achieved through using these low-temperature-synthesized and toxic ion-free IC-CNRs as solid phosphors on blue LED chips. This work demonstrates that the design of surface states plays a crucial role in exploring new functions of fluorescent carbon nanomaterials.*

White-light-emitting diodes (W-LEDs) have become an important energy-saving technique for the sustainable development of our society because of the virtues of long lifetime and low electricity consumption. Among various strategies of W-LEDs, integration of blue LED chips with yellow phosphors has been proven to be the most practical way. However, one of the reasons why the W-LED industry still needs governmental allowance is due to the expensive and ineluctable rare-earth raw materials for conventional phosphors.[1] Another newly developed strategy is quantum-dot- (QDs) based W-LEDs with tunable color characters. But, almost all of the high-performance QDs involve Pd^{2+} or Cd^{2+}, which is toxic.[2] Therefore, finding low-cost and environment-friendly substitutes for rare-earth-based phosphors or Pd^{2+}/Cd^{2+}-based QDs is crucial and still a great challenge for W-LEDs.

Fortunately, carbon, as one of the most abundant materials in our earth, was found to emit visible light when it was tailored into nanoscale materials, such as carbon nanodots. Significantly, its quantum yield was reported to be as high as 80%, which is even comparable with the best inorganic semiconductor QDs.[3] So, luminescent nanoscale carbon materials exhibit an outstanding potential for W-LEDs because of their low-cost and environment-friendly advantages. However, one serious obstacle seems to be fading such prospective roadmap. Currently, most visible luminescence from carbon dots (CDs) were observed in colloidal states, but aggregation-induced quenching (AIQ) effects usually occurred when drying them into films or powders.[3,4] Obviously, the absence of luminescence in the solid state has greatly limited the development of fluorescent carbon nanomaterials in W-LEDs.[5] As an alternative approach, we recently reported the incorporation of carbon dots into polymers to form composites and to preserve surface states, and hence obtain visible luminescence for W-LEDs.[6] But, without doubt, the best way is to achieve high-quality luminescence in the solid state for fluorescent carbon nanomaterials and then directly use these materials as phosphors in W-LED.

In this work, precursors and processes were elaborately designed to achieve the fabrication of intercrossed carbon nanorings (IC-CNRs) with very pure hydroxyl surface states for the first time, which enabled them to overcome AIQ effect, and to emit yellow-orange luminescence in both colloidal and solid states. Remarkably, although only a very simple and one-step hydrothermal process was implemented on poly(vinyl alcohol), PVA, very pure surface states, only hydroxy groups (unavoidable hydrogen was not taken into consideration), were formed on these IC-CNRs, which was confirmed by Fourier transform infrared spectroscopy (FTIR) and X-ray photoelectron spectroscopy (XPS) analyses. As a direct benefit of such scarce solid luminescence from IC-CNRs, they were used as low-cost and environment-friendly phosphors on blue chips, and hence W-LEDs were achieved

[*] X. Li,[+] Y. Liu,[+] Dr. X. Song, Prof. H. Zeng
State Key Laboratory of Mechanics and Control of Mechanical Structures &
College of Materials Science and Technology
Nanjing University of Aeronautics and Astronautics
Nanjing (China)
and
Institute of Optoelectronics & Nanomaterials
College of Materials Science and Engineering
Nanjing University of Science and Technology
Nanjing, 210094 (China)
E-mail: zeng.haibo@njust.edu.cn
Dr. H. Wang, Dr. H. Gu
Collaborative Innovation Center for Advanced Organic Chemical Materials &
Faculty of Physics and Electronic Science, Hubei University
Wuhan 430062 (PR China)
[+] These authors contributed equally to this work.

[**] Financially supported by National Basic Research Program of China (grant number 2014CB931700), NSFC (grant number 61222403), Doctoral Program Foundation of China (grant number 20123218110030), Opened Fund of the State Key Laboratory on Integrated Optoelectronics (grant number IOSKL2012KF06) and Fundamental Research Funds for the Central Universities (grant numbers 30920140121007, 30920130111017, and NE2012004).
Supporting information for this article is available on the WWW under http://dx.doi.org/10.1002/anie.201406836.

with optimized color coordinate of (0.28, 0.27), which is close to pure white light (0.33, 0.33).

Although the details of the luminescence mechanism are still in debate for fluorescent carbon nanomaterials, it has been widely recognized that the surface states and HOMO–LUMO emissions play their roles together. For example, Shang et al. suggested that the luminescence could be attributed to the electronic transitions between the pure and oxidized carbon regions, in which C−O, C=O, and O=C−OH groups participate.[7c] In addition, these plenty surface states give a chance for the colloidal CDs to adjust their luminescence. As a typical example, we recently reported the control of the excitation dependence of CD luminescence through the degree of surface passivation.[7a] On the other hand, the interaction between different surface states during drying samples can facilitate the AIQ behavior, which is similar to organic fluorescent dyes.[8] For luminescence-quenched carbon dots, usually there are various surface groups, which act as electron donors and acceptors. When the carbon dots aggregate (drying), these donors and acceptors form π-π stacking and induce the quenching of luminescence.[9]

Considering the above AIQ effect of surface states on the luminescence, if we can design and achieve a relatively pure surface, the donor–acceptor attraction among adjacent luminescent carbon nanounits would be greatly depressed, and hence luminescence in the solid state could be well persisted.[10] To achieve this hypothesis, we selected PVA as a precursor because it possesses only OH functional groups. Moreover, compared with small molecules, this linear polymer is more stable and cannot be oxidized easily, which is also important for the construction of relative pure surface state. The formation processes of IC-CNRs are shown in Figure 1. First, in a hydrothermal environment, a dehydration reaction was ready to take place through combining OH and H from two adjacent PVA molecular chains, as shown in Figure 1 (left), resulting in their bonding on the chain sides. Subsequently, the repetitious incorporation would form graphene ribbon-like structures, as shown in Figure 1 (middle). After that, due to the existence of residual active dangling bonds at the end of the chains, the ribbon-like carbon structures would crimp along the longitudinal direction, and even link the ends to form ring-like structures. Finally, the residual hydroxy groups on one ribbon would react with hydrogen on another one, which might result in the formation of intercrossed structures as shown in Figure 1 (right). When most of the hydroxy groups were consumed, the residual hydroxy groups located at the edges to form surface states. According to the above formation process, it is obvious that the surface states will mainly form by residual hydroxy groups and the steady intercrossing states can effectively restrain their aggregation. So, such unique IC-CNRs with very pure hydroxy surface states can be expected to overcome the AIQ effect, and to possess strong luminescence in the solid state. As shown in Figure S1, some intermediate states, including curved carbon ribbons and separated carbon nanorings, have been observed to support the above formation process well.

The designed microstructure and surface states of IC-CNRs have been well confirmed by a series of characterizations as shown in Figure 2 and Figure S2 (XPS spectra of CR-6 and CR-12). Figure 2a presents a TEM image of typical IC-CNRs. Several truths verify the intercrossing state. First, there is no doubt on their ring-like morphology as clearly revealed by TEM images (Figure 2a). Second, we have tried to separate them into isolated rings through sonication, but always failed. Furthermore, it can be discriminated that, for the upper ring segment, the corresponding imaging contrast is slightly larger than that of the underlying ring segment, indicating an intercrossing state of these two rings (detailed high-resolution transmission electron microscopy, HRTEM, images can be seen in Figure S3). Interestingly, their unique stacking state is moderate between aggregation and isolation, which can contribute to the depression of AIQ effect. Through analyzing more than 100 rings from the TEM pictures, we find that the distribution of outside diameter is very narrow (10–20 nm) and the average diameter is 15 nm (Figure 2b). But the average inner diameter is about 7 nm, which is much larger than typical carbon onions.[11] The HRTEM image, as shown in Figure 2c, validates the intercrossing state of IC-CNRs much clearer. At the same time, the observed lattice spacing of 0.35 nm is in accordance with the interlayer distance of graphite. Furthermore, the completely empty inners demonstrate that the formed products are IC-CNRs, but not carbon onions. Corresponding to the above narrow diameter distribution, their layer numbers are also very focused on 6–12 with an avarage layer number of 9, as shown in Figure 2d.

The surface groups were identified by FTIR and XPS spectra. Figure 2e shows the variation of surface groups on

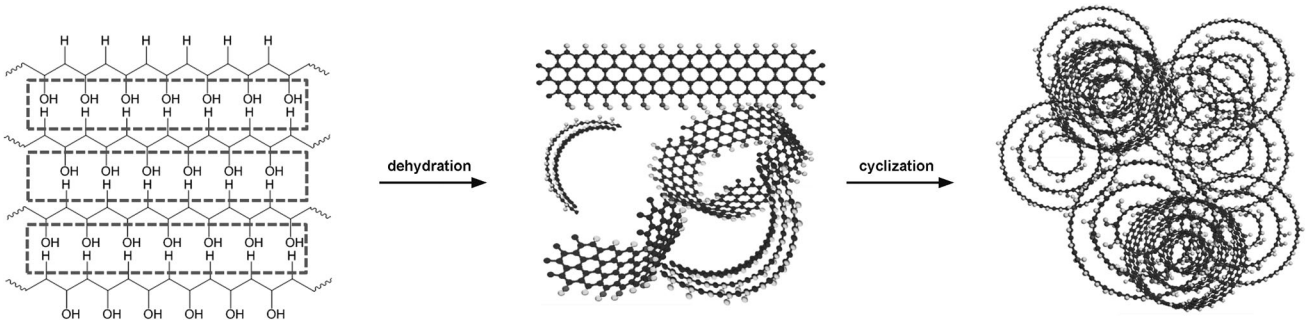

Figure 1. Schematic strategy proposed to form IC-CNRs and pure hydroxy surface states. Poly(vinyl alcohol) was used as precursor and suffered from dehydration and cyclization reactions during hydrothermal treatment.

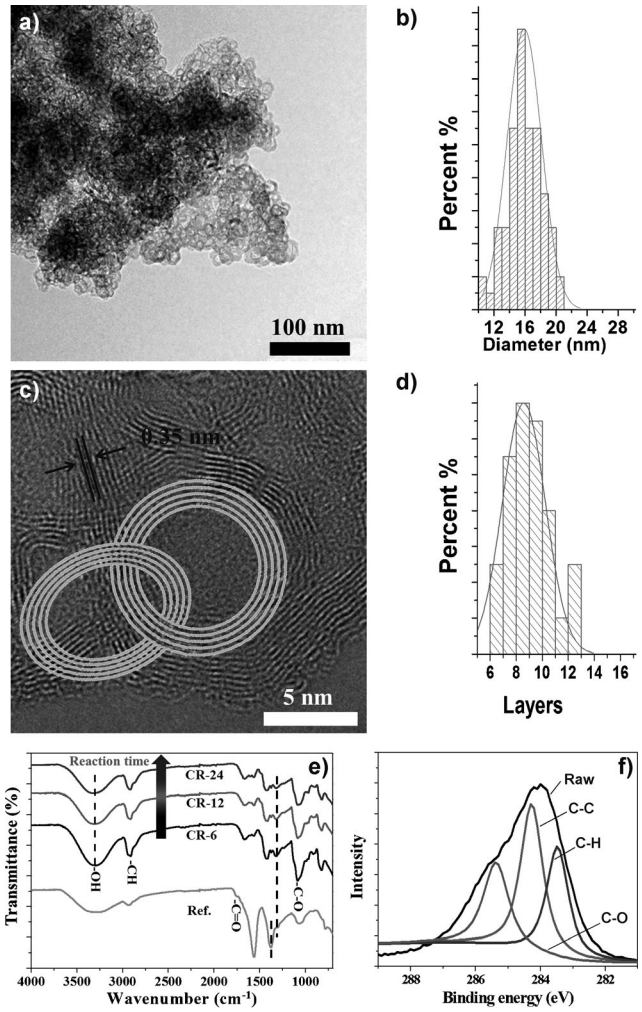

Figure 2. Characterizations of microstructure and surface state of formed IC-CNRs. a) TEM image of nanorings. b) Nanoring diameter distribution, showing average diameter of 15 nm. c) HRTEM image of nanorings, exhibiting 0.35 nm lattice spacing in well accordance with graphite. d) Atomic layer number distributions of nanorings, showing average layer number of 9. e) FTIR spectra of nanorings prepared with reaction time of 6 (CR-6), 12 (CR-12) and 24 h (CR-24). The reference sample is CR-24 after carbonization. f) C 1s XPS spectra of typical nanorings.

the hydrothermal reaction time. With increasing reaction time, no new IR peak appears, but the relative intensities of different peaks change obviously. The two strongest absorption band at 1087 and 3310 cm^{-1} are typical C–O stretching vibrations and OH groups. Interestingly, such abundant OH groups endow these carbon nanorings outstanding water solubility larger than $>60\ mg\,mL^{-1}$ and sustained colloidal stability more than one year without any sedimentation. Remarkably, the peak intensity of the hydroxy group decreases with the increase of the reaction time, which is due to further carbonization. Absorption bands at 2918, 2895, 1310, and 1422 cm^{-1} are asymmetric and symmetric stretching, out-of-plane, and in-plane bending vibrations of CH_2, respectively. Two absorption bands around 1600 cm^{-1} are stretching vibrations of C=C. Besides the hydroxy groups, there is no oxidation surface groups on the rings. Otherwise, the characteristic peaks are almost the same with PVA.[12] The spectrum of CR-24 after carbonization is also shown as a reference in Figure 2e. Peaks corresponding to carboxy groups at 1758 and 1376 cm^{-1} are observed, which are absent in the as-prepared samples. These IR characters demonstrate that a relatively pure surface has been constructed successfully, which is further confirmed by the surface-bonding states reflected by XPS spectra as shown in Figure 2f. There are no unsaturated chemical states for carbon atoms except for original bonds, such as C–O (285.2 eV), C–C (284.2 eV) and C–H (283.4 eV), which is well-consistent with FTIR spectra. Elemental analysis revealed that the ratio of C/O increased after a longer reaction time (Table S4). All the results confirm the pure surface states of the hydroxy groups.

To investigate the influence of purification of surface groups on optical properties, UV/Vis and PL measurement were conducted. Unlike previous reports of luminescent CDs,[17] no absorption peaks are observed for these IC-CNRs in the UV/Vis absorption spectra (Figure 3a) and the curves rise rapidly like semiconductors to form absorption edges. For CDs, there is usually an absorption peak at about 330 nm (as shown in Figure 3a), which is associated with the n-π^* transition from amino or carboxy groups.[7a,13] So, the absence of such absorption peak indicates that the relatively pure surface states without amino and carboxy groups have been formed through this method, which is in accordance with above FTIR and XPS results. Furthermore, the absorption edges redshift with the decrease of reaction time and the color of nanoring colloids changes from yellow to orange under a UV lamp irradiation.

The PL spectra show an optimal emission peak at 540 nm when excited at 420 nm (Figure 3b). The same redshift of optimized PL behavior is observed in samples prepared with different time. Such redshift can be assigned to the different amount of hydroxy groups as confirmed by FIIR and XPS spectra. As electron-donating groups, they can reduce the HOMO–LUMO energy gap, resulting in the red-shifted PL and absorption behavior.[14] In addition, they exhibit excellent fluorescent stability under the illumination of a UV lamp (350 nm, 20 W) for 16 h (Figure S6). Interestingly, all the IC-CNRs exhibit excitation-dependent and excitation-independent PL behavior at the same time (Figure 3c and S7). That is, the evolution of their emissions with excitation wavelengths can be separated into two regions, which is seldom observed.[14,15] For CR-6, as an example, when it is excited at wavelengths between 320 to 400 nm, the emission peaks keep their positions unchanged and just increase in intensities. However, the emissions red-shift and become weaker with the increase of excitation wavelengths when they are larger than 400 nm. The excitation dependence of the PL, first observed at 528 nm and then at more than 565 nm, has been well plotted in Figure 3d. Actually, no absorption and photoluminescence is observed for the PVA aqueous solution (Figure S8), which demonstrates that the observed optical properties originate from the synthesized IC-CNRs.

Recently, luminescence-dependent and independent behaviors were reported for partially and totally passivated CDs.[7a] The luminescence origin can be attributed to the electronic transitions from the bottom of the LUMO and the

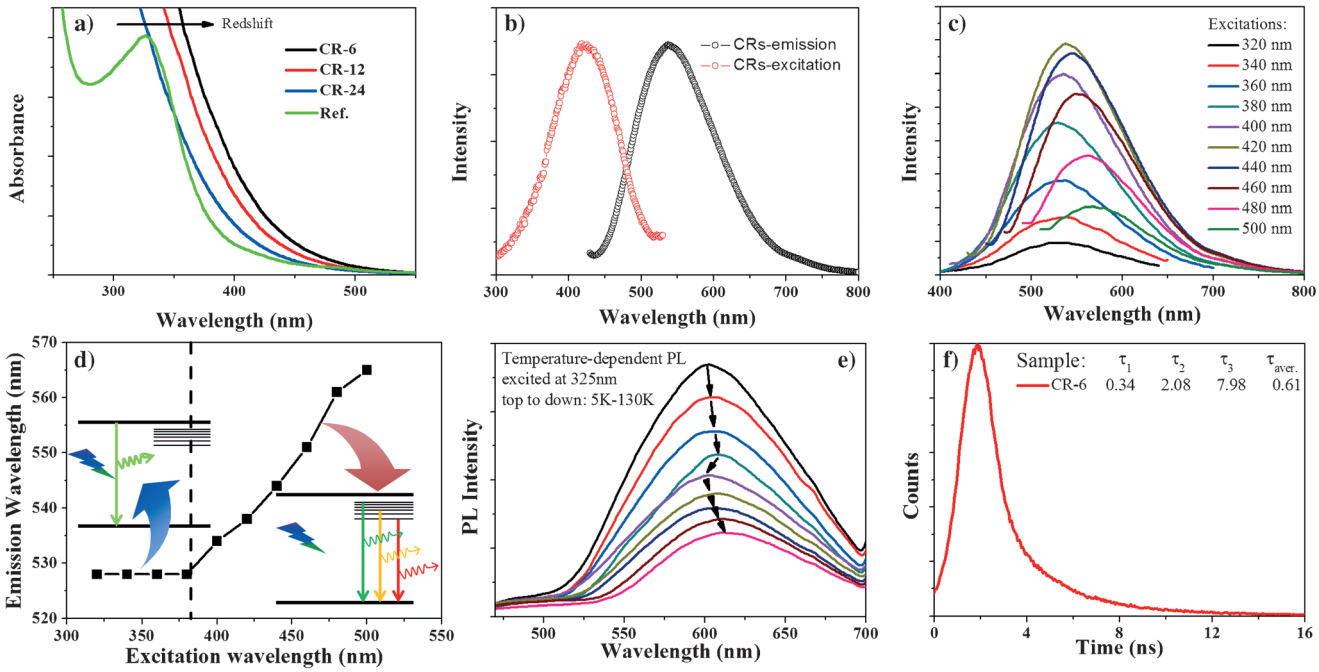

Figure 3. Photoluminescence properties of IC-CNRs. a) UV/Vis spectra of IC-CNRs aqueous solutions prepared under 6, 12, 24 h and carbon dots from Ref. [7a]. b) PL spectrum of CR-6 excited at 420 nm and the corresponding PL spectrum. c) PL emission under different excitation wavelength. d) PL emission wavelength maxima versus excitation wavelength. The inset shows the proposed luminescence mechanism. e) Temperature-dependent PL spectra of CR-6 from 5 to 130 K at 325 nm excitation. f) PL lifetime spectra of CR-6.

nearby states to the HOMO as shown in the inset of Figure 3d. Abundant surface groups of CDs introduce many energy levels in the energy gap and these multiple electronic transitions lead to excitation-dependent behavior because different transition modes dominate under different excitations. Generally, the variation of emission wavelength under different excitations is often larger than 70 nm because different surface groups affect many energy levels.[7a,16] Obviously, if the surface is pure, there will be less energy levels and the energy interval will be narrow. Therefore, the variation of emission wavelength will be small. The PL results in this work agree well with our proposed mechanism. As there is only one kind of surface group in this work, the PL emission wavelength changes from 528 to 565 nm (37 nm, shown in Figure 3d), which is much narrower than most of the reports. After oxidation with potassium permanganate, the maximum emission wavelength shifted to a shorter wavelength and carboxy groups were observed from the FTIR spectrum (Figure 2e). Importantly, the variation of emission wavelength increases to 90 nm (Figure S9). It confirms that pure hydroxy groups make great contributions to PL features and when other groups are introduced, the optical properties change.

Interestingly, the IC-CNRs still emit light upon drying as expected. The solid-state luminescence can be attributed to following facts. First, as we mentioned above, complex surface groups make them electron donating and accepting, resulting in nonradiative photoinduced electron transfer. Here, we give an example that C-LMs can possess pure surface groups and stable luminescence is obtained in both solid and aqueous phases because of the depression of the quenching effect. Second, from the TEM images (inset in Figure 2c) we can see that the carbon nanorings are intercrossed. Such intercrossed behavior makes the rings support each other, reducing the possibility of complete aggregation. Last but not least, structure properties of the IC-CNR powder samples were characterized using XRD and the patterns of the samples exhibit two characteristic peaks of PVA (Figure S10). Due to the strong intensity originating from PVA, the information of IC-CNRs is covered because the peaks of carbon materials localize at similar sites. When increasing the reaction time, the peak intensities decrease with the reduction of the PVA content. This indicates that the IC-CNRs keep the luminescent state and act like IC-CNR/PVA composites, which still can emit light upon drying. PVA rich of OH groups studied by FTIR and XPS also support this observation.

Importantly, solid-state emission makes temperature-dependent PL measurement possible. To gain more insight into the effects of pure surface states on the PL, a combination of temperature-dependent PL and time-correlated single-photon counting (TCSPC) were performed. The broadening of the emission peak for slices made from powders compared with that of IC-CNRs in aqueous solutions may be caused by an inner filter effect and energy transfer within an inhomogeneous distribution emitting species embedded in the solid state.[17] Localized electronic states are observed because the PL exhibited a sudden blue-shift from 20 to 30 K (Figure 4a), which is frequently observed in typical semiconductors.[18] However, it is only found in theoretical calculations[7c] and is seldom observed experimentally in carbon materials.[19] Structurally, these localized states are probably from fluorophore structures and consist of carbon nanoring structures

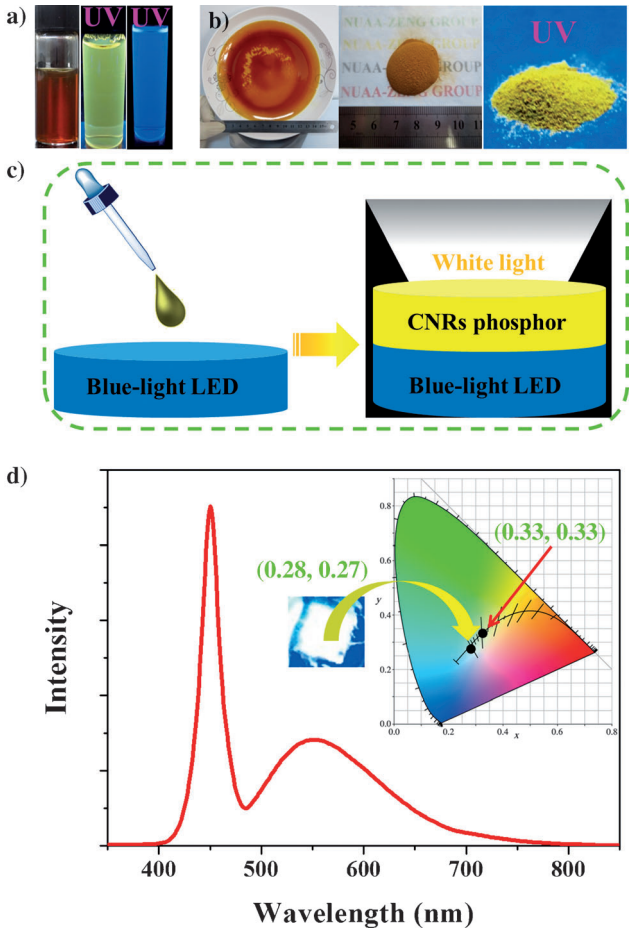

Figure 4. Applications of carbon nanoring phosphors in W-LEDs. a) IC-CNRs and carbon dots (Ref. [7a]) dispersions under sunlight and UV light. b) Images of film and powders under sunlight and UV light. c) Fabrication strategy of W-LEDs based on blue-light-emitting diodes. d) Electroluminescence (EL) spectra of assembled LED. The insets are the digital image of the device and the corresponding CIE (Commission internationale de l'éclairage) chromaticity diagram.

and OH groups. Figure 3 f shows the PL decay curve of CR-6 and the resultant average lifetime is 0.61 ns, containing three lifetime components: 0.34 ns, 2.08 ns, and 7.98 ns, respectively. The multiple exponential PL decay was caused by different emission states of band-edge and localized electronic states. The decay curves of three samples are similar (Figure S11). All the results are consistent with the proposed mechanism that luminescence originates from the transition between multiple excited states (LUMO, medium states) and HOMO.

As shown in Figure 4, the purified surface states donate the IC-CNRs luminescence in the solid state, and hence they are acting as phosphors for W-LED. Figure 4 a shows the digital images of IC-CNRs dispersions under sunlight and UV light irradiation, exhibiting obvious yellow luminescence in the colloidal state. Figure 4 b shows the typical film and powders of IC-CNRs under sunlight and UV light, exhibiting luminescence in the same yellow color in the solid state. Moreover, the large yield of the synthesis of IC-CNRs can be verified by Figure 4 a and b. Figure 4 c shows the preparation process of the device with LED chip and IC-CNRs phosphors. An IC-CNRs solution was dropped onto the LED chip and then dried into the solid films. This process was repeated for several times. The emission spectrum of the device was measured and is shown in Figure 4 d, which contains two components. The first one is from the chip centered at about 460 nm. Another emission band is from IC-CNRs because similar PL peak position and shape have been observed from IC-CNRs colloids under 460 nm excitation (Figure 3 c). White light is clearly observed from the device with IC-CNRs phosphors, as shown in the inset of Figure 4 d. The color characters of luminescence from such devices were analyzed by CIE 1931 chromaticity coordinates. The coordinate is realized at (0.28, 0.27), which is close to the pure white coordinate (0.33, 0.33). Though few LED applications have been demonstrated recently, most of them employed composites combining polymers and CDs to preserve the surface states and luminescence.[20] However, the introduction of a thick polymer layer will depress the luminescence from chips and also increase the costs. Here, this is the first report to demonstrate the direct application of luminescent carbon nanomaterials as phosphors for W-LEDs. Furthermore, compared with high-temperature synthesized phosphors containing expensive rare-earth elements, carbon materials are cost-effective and the solution process is also low-cost and compatible with printing devices. Therefore, such low-temperature solution-processed carbon nanorings showing luminescence in solid state could have wide applications in future printing LEDs.

Another interesting phenomenon is the pH-dependent behavior of these IN-CNRs. The photoluminescence intensities decrease in solutions with high or low pH value, while they almost keep stable when the pH is changed from 5 to 12 (Figure S12). Moreover, strong room-temperature magnetism can be observed after carbonization in nitrogen atmosphere (Figure S13), which may be attributed to magnetic zig-zag edge states.[21] The interesting physical properties and structure features are consistent with the proposed reaction processes. Additionally, the present method can also be applied to other linear polymers, such as polyacrylic acid (PAA) and polyacrylamide (PAM) (Figure S16), to fabricate luminescent carbon-based materials.

In summary, we have demonstrated a one-step hydrothermal method for the fabrication of IC-CNRs for the first time. Relatively pure surface states were constructed and stable luminescence was achieved in both solid and aqueous states by reducing the interaction between different luminescent nanounits. Aggregation-induced quenching was depressed successfully and the IC-CNRs were applied as inexpensive phosphors in W-LEDs. Microstructure measurement confirmed the pure surface states and optical properties changed immediately when oxidization groups were introduced. Such pure surface states resulted in narrow energy levels between the energy gap and a smaller variation of emission wavelength (about 37 nm) was observed. The surface groups behaved like intrinsic defects in inorganic semiconductors and localized states were observed experimentally in temperature-dependent PL measurement. Investigations proved that the luminescence can be attributed to the

electronic transitions from the bottom of the LUMO and the nearby localized states to the HOMO.

Experimental Section

Preparation of intercrossed carbon nanorings: Polyvinyl alcohol (PVA, 1 g, Mw: 1750) was dissolved in 20 mL distilled water. Then, a certain amount of sodium hydroxide was added to accelerate the carbonization and polymerization. Thereafter, the transparent solution was transferred to a Teflon autoclave and heated at 250 °C for 6, 12, and 24 h, the samples being further denoted as CR-6, CR-12, and CR-24, respectively. When the reaction finished, the reactors were cooled to room temperature naturally. The obtained solutions were centrifuged at 10 000 rpm for 10 minutes to remove the large particles. Then, the brown solutions were dialyzed against distilled water through a dialysis membrane (Da = 3000) for three days to remove unreacted materials. The water was changed every 8 h. Finally, the solutions were dried under vacuum at 70 °C for 48 h in a china dish. The formed film was scraped and made into powders.

Characterizations: X-ray diffraction (XRD) patterns were recorded on a multipurpose XRD system D8 Advance from Bruker with a $Cu_{K\alpha}$ radiation. UV/Vis absorption spectra were obtained using a Shimadzu 3600 UV/Vis spectrophotometer and photoluminescence (PL) spectra were measured with a Varian Cary Eclipse instrument. HRTEM images were recorded on FEI Tecnai F30 S-TWIN. Fluorescence lifetimes were measured using a Horiba FM-4P time-corrected single-photon-counting (TCSPC) system. The temperature-dependent photoluminescence spectra were measured at Horiba luminescence spectrometer (HR 320) with a laser excitation at different temperatures. FTIR spectra were recorded with a Tensor-27 spectrometer. XPS analysis was carried out on an ARL-9800 instrument with monochromatic X-ray source $Al_{K\alpha}$ excitation (1486.6 eV). Raman-shift spectra were measured on a JY HR800 tool with laser excitation of 488 nm. The white-light LED was fabricated with a GaN-based blue LED chip (λ peak = 460 nm).

Received: July 3, 2014
Revised: July 31, 2014
Published online: September 11, 2014

Keywords: carbon · luminescence · nanorings · surface states · white-light-emitting diodes

[1] a) J. K. Park, C. H. Kim, S. H. Park, H. D. Park, S. Y. Choi, *Appl. Phys. Lett.* **2004**, *84*, 1647; b) H. He, R. Fu, Y. Cao, X. Song, Z. Pan, X. Zhao, Q. Xiao, R. Li, *Opt. Mater.* **2010**, *32*, 632.
[2] J. Chen, D. Zhao, C. Li, F. Xu, W. Lei, L. Sun, A. Nathan, X. W. Sun, *Sci. Rep.* **2014**, *4*, 4085.
[3] S. J. Zhu, Q. N. Meng, L. Wang, J. H. Zhang, Y. B. Song, H. Jin, K. Zhang, H. C. Sun, H. Y. Wang, B. Yang, *Angew. Chem. Int. Ed.* **2013**, *52*, 3953; *Angew. Chem.* **2013**, *125*, 4045.
[4] S. N. Qu, X. Y. Wang, Q. P. Lu, X. Y. Liu, L. J. Wang, *Angew. Chem. Int. Ed.* **2012**, *51*, 12215; *Angew. Chem.* **2012**, *124*, 12381.
[5] a) P. Yu, X. Wen, Y. R. Toh, J. Tang, *J. Phys. Chem. C* **2012**, *116*, 25552; b) F. Wang, S. Pang, L. Wang, Q. Li, M. Kreiter, C. Y. Liu, *Chem. Mater.* **2010**, *22*, 4528; c) Y. X. Fang, S. J. Guo, D. Li, C. Z. Zhu, W. Ren, S. J. Dong, E. K. Wang, *ACS Nano* **2012**, *6*, 400.
[6] a) P. Zhang, W. C. Li, X. Y. Zhai, C. J. Liu, L. M. Dai, W. G. Liu, *Chem. Commun.* **2012**, *48*, 10431; b) Y. H. Deng, D. X. Zhao, X. Chen, F. Wang, H. Song, D. Z. Shen, *Chem. Commun.* **2013**, *49*, 5751; c) Z. Xie, F. Wang, C. Y. Liu, *Adv. Mater.* **2012**, *24*, 1716.
[7] a) X. M. Li, S. L. Zhang, S. A. Kulinich, Y. L. Liu, H. B. Zeng, *Sci. Rep.* **2014**, *4*, 4796; b) S. L. Hu, K. Y. Niu, J. Sun, J. Yang, N. Q. Zhao, X. W. Du, *J. Mater. Chem.* **2009**, *19*, 484; c) J. Z. Shang, L. Ma, J. W. Li, W. Ai, T. Yu, G. G. Gurzadyan, *Sci. Rep.* **2012**, *2*, 792; d) L. Bao, Z. L. Zhang, Z. Q. Tian, L. Zhang, C. Liu, Y. Lin, B. Qi, D. W. Pang, *Adv. Mater.* **2011**, *23*, 5801.
[8] S. F. Xie, S. X. Bao, J. J. Ouyang, X. Zhou, Q. Kuang, Z. X. Xie, L. S. Zheng, *Chem. Eur. J.* **2014**, *20*, 5244.
[9] H. T. Li, X. D. He, Z. H. Kang, H. Huang, Y. Liu, J. L. Liu, S. Y. Lian, C. H. A. Tsang, X. B. Yang, S. T. Lee, *Angew. Chem. Int. Ed.* **2010**, *49*, 4430; *Angew. Chem.* **2010**, *122*, 4532.
[10] G. E. LeCroy, S. K. Sonkar, F. Yang, L. M. Veca, P. Wang, K. N. Tackett, J. J. Yu, E. Vasile, H. J. Qian, Y. M. Liu, P. J. Luo, Y. P. Sun, *ACS Nano* **2014**, *8*, 4522.
[11] D. Pech, M. Brunet, H. Durou, P. Huang, V. Mochalin, Y. Gogotsi, P. L. Taberna, P. Simon, *Nat. Nanotechnol.* **2010**, *5*, 651.
[12] S. J. Zhu, J. H. Zhang, L. Wang, Y. B. Song, G. Y. Zhang, H. Y. Wang, B. Yang, *Chem. Commun.* **2012**, *48*, 10889.
[13] a) X. H. Zhu, X. Xiao, X. Y. Zuo, Y. Liang, J. M. Nan, *Part. Part. Syst. Charact.* **2014**, *31*, 801; b) D. Qu, M. Zheng, P. Du, Y. Zhou, L. G. Zhang, D. Li, H. Q. Tan, Z. Zhao, Z. G. Xie, Z. C. Sun, *Nanoscale* **2013**, *5*, 12272.
[14] H. Z. Zheng, Q. L. Wang, Y. J. Long, H. J. Zhang, X. X. Huang, R. Zhu, *Chem. Commun.* **2011**, *47*, 10650.
[15] a) W. Sun, Y. X. Du, Y. Q. Wang, *J. Lumin.* **2010**, *130*, 1463; b) S. Chandra, P. Patra, S. H. Pathan, S. Roy, S. Mitra, A. Layek, R. Bhar, P. Pramanik, A. Goswami, *J. Mater. Chem. B* **2013**, *1*, 2375.
[16] Y. P. Sun, B. Zhou, Y. Lin, W. Wang, K. A. S. Fernando, P. Pathak, M. J. Meziani, B. A. Harruff, X. Wang, H. F. Wang, P. G. Luo, H. Yang, M. E. Kose, B. Chen, L. M. Veca, S. Y. Xie, *J. Am. Chem. Soc.* **2006**, *128*, 7756.
[17] F. Wang, M. Kreiter, B. He, S. P. Pang, C. Y. Liu, *Chem. Commun.* **2010**, *46*, 3309.
[18] H. B. Zeng, Z. G. Li, W. P. Cai, P. S. Liu, *J. Appl. Phys.* **2007**, *102*, 104307.
[19] G. Schubert, H. Fehske, *Phys. Rev. Lett.* **2012**, *108*, 066402.
[20] a) Q. L. Chen, C. F. Wang, S. Chen, *J. Mater. Sci.* **2013**, *48*, 2352; b) W. Kwon, S. Do, J. Lee, S. Hwang, J. K. Kim, S. W. Rhee, *Chem. Mater.* **2013**, *25*, 1893; c) W. Kwon, G. Lee, S. Do, T. Joo, S. W. Rhee, *Small* **2014**, *10*, 506.
[21] C. G. Tao, L. Y. Jiao, O. V. Yazyev, Y. C. Chen, J. J. Feng, X. W. Zhang, R. B. Capaz, J. M. Tour, A. Zettl, S. G. Louie, H. Dai, M. F. Crommie, *Nat. Phys.* **2011**, *7*, 616.

